A LUMPED MODEL OF DOUBLE SKIN FACADE WITH CAVITY SHADING

Yuan Yuan[1], Jianlong Zeng[2], Yingxin Zhu[2], Borong Lin[2]

[1]Department of Architecture, University of Pennsylvania, PA19104, USA
[2]Department of Building Science, School of Architecture, Tsinghua University, Beijing 10084, China

ABSTRACT

A universal lumped model is developed with the aim to predict the thermal performance of Double Skin facade. Three modules – ventilation, heat transfer and penetration - are coupled to comprehensively describe the energy and mass transfer processes. The unknown parameters, resistance coefficient and heat convection coefficient, are discussed and estimated. The influences of cavity shading position, cavity depth and ventilation height on energy performances are analyzed at the end of the paper based on the simulation results.

KEYWORDS

Double Skin Facade, Thermal Performance, Lumped Model, Ventilation, Resistance Factor

INTRODUCTION

The complexity of Double Skin Facade (DSF) design results from the interaction of various factors, such as the structure, glass property, building orientation and location. Therefore, to achieve a desirable thermal performance, assisting simulations is usually indispensable. Two kinds of simulation methods are widely used – Lumped Parameters and Computational Fluid Dynamic (CFD). Most DSF studies now are based on CFD simulation (Dirk 2001, R.Letan 2002, Manz, H. 2004, Malkawi A. 2004). However, although CFD is highly valued in research field, professional knowledge and abundant simulation experiences are required in order to obtain a correct result, which limits its application by architects. Aiming to provide a more generally applicable model, former researchers also developed some lumped models [Carla 2002, Park 2004]. The common deficiency of existing lumped models is that they are unable to take into account the cavity shading, which actually plays the vital role in determining the energy performance of DSF.

To take a further step by adding cavity shading into the existed lumped models, three problems should be considered.

(1) The resistance coefficients change with the position of shadings;

(2) The heat convection coefficients enhanced by the additional heat surfaces, such as window frames and shading devices;

(3) The optical property of DSF as a multi-layer subtransparent system.

The aim of this work is to build a simplified but universal two dimensional lumped model, involving in the cavity shading devices. Particular attentions are paid to the three problems mentioned above.

PHYSICAL MODEL

A ventilated DSF usually consists of two transparent glass layers and in-between shading device which divide the cavity into two channels. Generally two opening are used for the cavity ventilation. Fig 1 shows a typical naturally ventilated DSF. In the lumped model, the input parameters are geometrical parameters, cavity ventilation strategy, glazing properties and shading type. The boundary conditions are indoor air temperature and outdoor weather data. Three modules are included and coupled calculated, describing the heat transfer, ventilation and penetrating process, respectively. All the physics processes are assumed to be steady state. The inputs, outputs and their logic relationship are show in Fig 2.

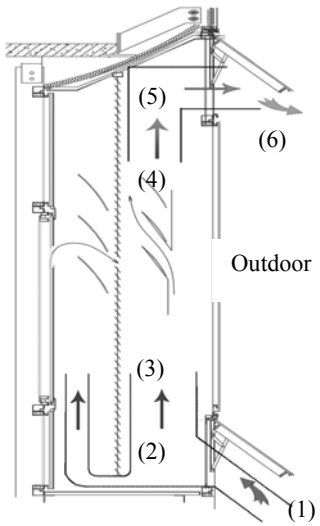

Fig 1 Typical DSF sketch

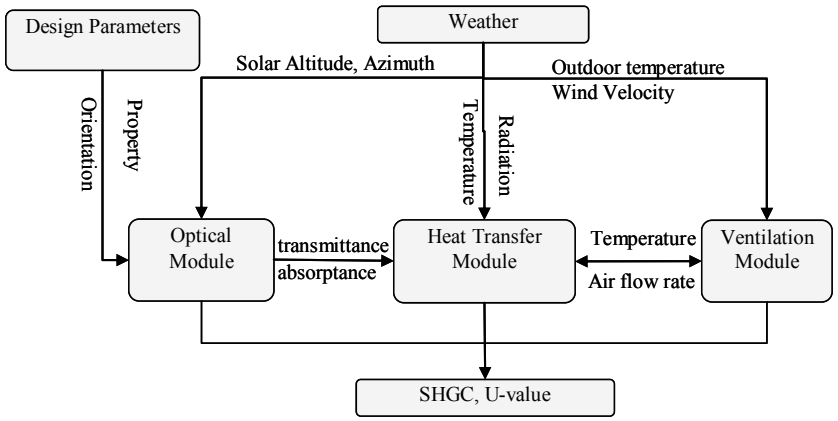

Fig 2 Schematic diagram

Ventilation Module

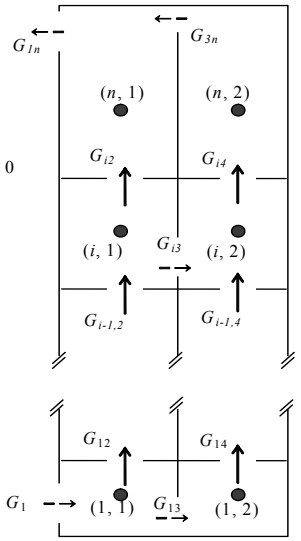

Fig 3 Ventilation network

Multi-zone airflow network is introduced to calculate the mass transfer through shading devices. Shown as *Fig 3*, the cavity is divided into *2n* calculation regions. The out-side channel connects with outdoor through facade openings. It is assumed that the air parameters are unique in each region and thus energy loss only happens when air flows from one region to another. Take the i^{th} ($i \neq 1$ or n) region in out-side channel as an example. The basic physic functions are

$$r_{(i,1)} = M_{(i-1,1)\to(i,1)} - M_{(i,1)\to(i+1,1)} - M_{(i,1)\to(i,2)} = 0 \quad (1)$$

$$M_{(i-1,1)\to(i,1)} = v_{(i-1,1)\to(i,1)} \rho_{(i,1)} Area_{(i-1,1)\to(i,1)} \quad (2)$$

$$P^{x}_{(i-1,1)} - P_{(i,1)} = P_{(i-1,1)} - \rho_{(i-1,1)} g\left(z^{x}_{i-1,1} - z_{i-1,1}\right) - P_{(i,1)} = \zeta_{(i-1,1)\to(i,1)} \frac{\rho_{(i,1)} v^{2}_{(i-1,1)\to(i,1)}}{2} \quad (3)$$

where M and P are the mass flow rate and static pressure, respectively. v is the velocity and ρ represents the air density. Equation (1) concerns about mass conservation. Equation (3) represents the relationship between airflow rate and pressure difference, evaluated by resistance coefficient ζ. When the ventilation is assisted by exhausting fan (mechanical ventilation), an extra pressure difference should be added to the top opening.

Resistance coefficients are not easy to be accurately determined, especially in the natural ventilation condition. Generally, CFD simulations or scale experiments are necessary to get the coefficient curve for each form of air path. However, a more universal method to obtain the rough values is to analog the DSF components with typical pipe components and thus to apply the existing pipe empirical function directly. For instance, the cavity channels can be regarded as two rectangular pipes, while the blinds can be simplified into numerous of tee branches. Take an example of a typical naturally ventilated DSF shown as Fig 1. Choose the out-side channel dimension as 0.5 (depth) × 3m (height), then the equivalent pipe components and resistance coefficients are shown in Table 1.

Table 1 Resistance Coefficients

Air path in DSF	(1) -> (2)	(2) -> (3)	(3) -> (4)	(4) -> (5)	(5) -> (6)	TOTAL
Equivalent Pipe Components	Up-hanging window	Tee Branch	Friction	Elbow	Up-hanging window	
Resistance Coefficient (Qingyao Lu. 1987)	9.25	1	0.5	2	9.25	22

Heat Transfer Module

In the heat transfer module, the DSF is divided into *7n* control volumes with n layers in height and 7 layers in depth. *Fig 4* shows the primary energy transfer processes happened in the i[th] layer. Steady state energy and mass balance equations give

Surface energy balance

$$h_{i,j}\left(T_{i,j-1}-T_{i,j}\right)+k_j\left(T_{i,j+1}-T_{i,j}\right)$$
$$+\sum_k \sigma_{i,j\to k}A_i\left(T_k^{\,4}-T_{i,j}^{\,4}\right)+I_{i,j}=0$$

Air mass & energy balance

$$h_{j\to j-1}\left(T_{i,j-1}-T_{i,j}\right)+h_{j\to j+1}\left(T_{i,j+1}-T_{i,j}\right)$$
$$+\rho C_p\left(G_{i-1,j}T_{i-1,j}+G_{i,j\pm1}T_{i,j\pm1}+G_{i,j}T_{i,j}\right)=0$$

Where T is the temperature, h, k and σ are convection heat transfer, conduction heat transfer coefficient and Stefan-Boltzmann constant, respectively. The subscript i and j represent the layer number in height and in depth respectively.

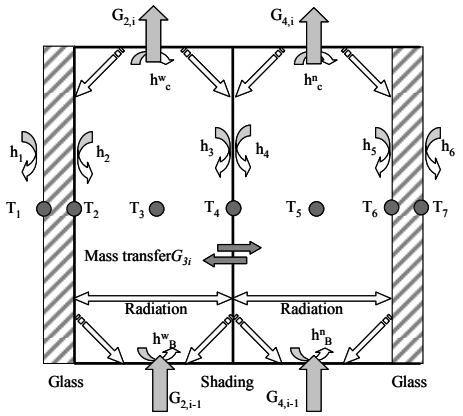

Fig 4 Heat transfer schematic diagram

The outdoor heat transfer coefficient (h_1) is given by Park (2004), and indoor heat transfer coefficient (h_6) is calculated according to ASHRAE handbook (2001).

$$h_1 = 5.68\left(0.92+\left(\frac{V}{0.3}\right)^{0.46}\right)$$

$$h_6 = 1.46\left[\frac{\left(T_7-T_{in}\right)}{H}\right]^{0.25}+e\sigma\left(T_7-T_{in}\right)$$

The convection heat transfer coefficient for the air inside the cavity is more complex. When the temperature difference ranges from 2 to 4ºC, a comparison functions from ASHRAE (2001) and the fitting function given by Park (2004) is shown in *Fig 5*. The noticeable gap between empirical and fitting functions implies that the convection heat transfer coefficient in cavity is not simply determined by temperature differences as empirical functions suggested, but greatly influenced by other disturbances, such as window frames and shading devices. To integrate all the influential factors, a modified Nusselt number formula is defined as follow.

$$Nu_{DSF} = C_M Nu_{em} = C_A C_T C_H Nu_{em}$$

Where

$$C_A = \frac{A_{glass}+A_{frame}}{A_{facade}} \geq 1$$

$$C_T = \frac{A_{glass}\Delta T_{glass}+A_{frame}\Delta T_{frame}}{\left(A_{glass}+A_{frame}\right)\Delta T_{glass}} \geq 1$$

$$C_H \geq 1$$

C_A describes the extra area introduced by window frames and shadings. C_T averaged the temperatures of transparent and opaque surface. C_H presents transfer enhancement due to the existing of disturbances (frame and shading). According to the experiments conducted by the author (2006), the value of C_H is generally between 1 to 2, depending on the distribution and the size of disturbances.

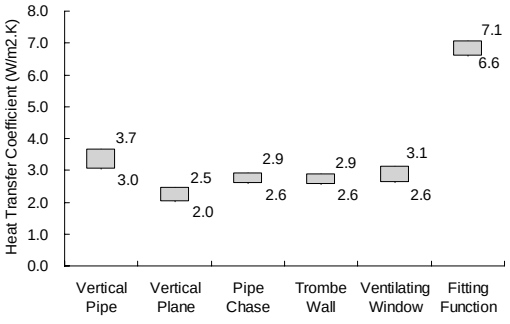

Fig 5 Comparison of Heat Transfer Coefficient Formulas

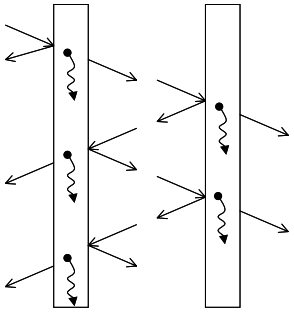

Fig 6 Light Path in multi-transparent system

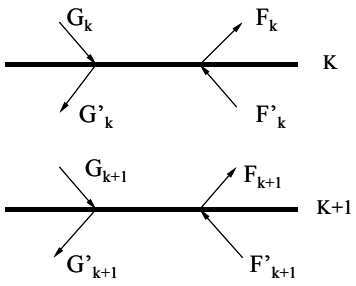

Fig 7 Surface energy balance

Penetration Module

The transmittance of each layer (glasses and shadings) in a multi-layer transparent system is no longer equals to its nominal value, but coupled with others. Therefore the transmittance of DSF is the infinite sum of components resulted from the multiple reflecting, absorbing and penetrating (*Fig 6*).

Yi Jiang (1980) proposed a general recursion formula in the base of energy balance. Any surface K (two surfaces for each layer) in the multi-layer system accepts energy G_K, shown as *Fig 7*. For every surface, the energy balance gives that the energy accepted by the surface equals the energy ejected, or written as

$$G_K^{'} + F_K = G_K + F_K^{'}$$

Moreover, if the media between two layers, say K and K+1, is glass instead of air, part of the energy is absorbed and conversed into thermal energy, which can be expressed as

$$\frac{G_{K+1}}{G_K^{'}} = \alpha_{K \to K+1}$$

The recursion formula of the transmittance of each layer is obtained by coupling the equations mentioned above.

RESULTS

To estimate the accuracy of the described model, a case study of an east facing naturally ventilated DSF is conducted based on the boundary conditions given by the experiments of the author (Yuan, 2006). The studied DSF locates in Beijing, China, with a dimension of 0.8 (Depth) × 5.6 (Width) × 3.0m (Height). The external glass is chosen as 6mm single glazing and the internal glass as Low-E glazing with U-value of 1.9W/(m^2.K) and SHGC[1] of 0.5. Light blind shading is installed in the cavity. Given the outdoor temperature of 25°C, the peak facade solar radiation of 600 W/m^2 and the indoor temperature of 24°C, *Fig 8* and *Fig 9* show the comparison between simulated and experimental result. According to the comparison, the maximum temperature error of the calculated value on the experimental one is less than 25%. The error of airflow rate shown in *Fig 9* is around 25%. The reasons resulting in the errors may be the insufficient recognition on the cavity air flow pattern and the mass exchange between two channels.

To get some more practical conclusions, the orientation of the study case is adjusted to south facing. Choose July 15th as a typical summer day. The input hourly climate data are given by the database of DeST. *Fig 12* presents the influence of blind position on SHGC. The blind position is defined as the ration of the distance from blind to out-side glazing on the total depth. *Fig 12* indicates that to minimize the value of SHGC, the optimal blind position is time dependent. However, *Fig 13* shows a monotone

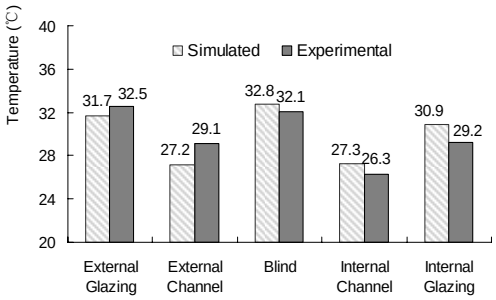

Fig 8 Comparison on Temperature

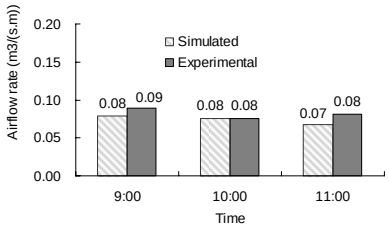

Fig 9 Comparison on Airflow rate

[1] SHGC: Solar Heat Gain Coefficient. It is the fraction of the incident irradiance that enters through the glazing and becomes heat gain.

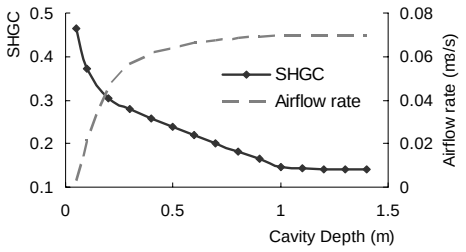

Fig 10 The influence of cavity depth

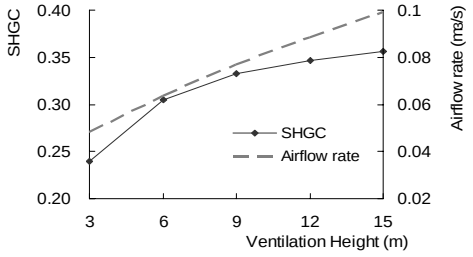

Fig 11 The influence of ventilation height

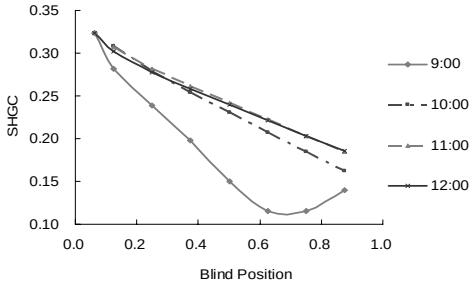

Fig 12 SHGC versus blind position

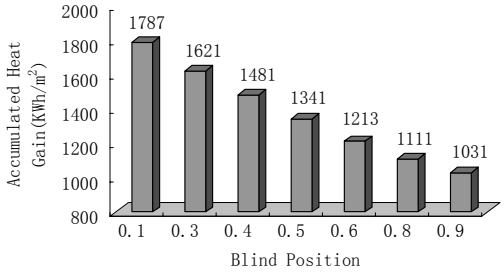

Fig 13 Whole-day heat gain versus Blind position

decreasing of the whole-day accumulated heat gain with the increase of blind position, which suggests that 40% heat gain can be reduced by placing the blind close to the in-side glazing.

Fig 10 shows the impact of cavity depth on SHGC. Generally SHGC reduces with the increasing of cavity depth. However, the simulation result indicates that SHGC goes down sharply when the depth changes from 0 to 0.2m, and then decreases smoothly when the depth is between 0.2 and 1m. When the cavity depth keeps increasing over 1m, the decrease of SHGC becomes inconspicuous.

Fig 11 shows the SHGC and airflow rate change with the ventilation height. Although the stack effect is enhanced by the increase of ventilation height, SHGC and cavity temperature goes up obviously. Therefore, to improve the thermal performance of DSF in summer, it is suggested to reduce the ventilation height or in other words, to increase the numbers of facade openings.

CONCLUSION

A steady-state universal lumped model is built to evaluate the thermal performance of DSF. The comparison between simulated and experimental data shows that the model can predict the performance accurately enough as a design assisting tool. The results of case study give that for naturally ventilated DSF, it is possible to reduce 40% of the heat gain in summer by place the cavity shading close to the in-side glazing. Further improvements on energy performance can be achieved by increasing the cavity depth if the depth is less than 1m or reducing the ventilation height. This model is also helpful to analyze and improve the energy performance of existing DSF. Further research can focus on the verification of the form resistance coefficients of different openings and the influence of wind pressure.

REFERENCES

Dirk Saelens and Hugo Hens. October 2001. Experimental evaluation of airflow in naturally ventilated active envelopes, Journal of thermal env. & bldg. sci., vol.25

R.Letan. 2002, Passive ventilation and heating by natural convection in a multi-storey building, Building and Environment

Manz, H., Schaelin, A. and Simmler, H.. 2004. Airflow patterns and thermal behavior of mechanically ventilated glass double facades. Building and Environment, 39:1023-1033

Malkawi, A. and Y. Yi. 2004. Simulating the Multi-Variables Effect on Double-Skin Facades. In Proceedings of the Eighth World Renewable Energy Congress (WREC), Boulder, Colorado

Carla Balocco. 2002. A simple model to study ventilated facades energy performance. Energy and Building, 34:469-475

Park Cheol-Soo and Augenbroe Godfried. 2004. Calibration of a lumped simulation model for double-skin facade systems. Energy and Buildings, 36:1117-1130

ASHRAE Fundamental Handbook. 2001. Chapter 2 Fluid Flow, Atlanta: American Society of Heating, Refrigerating, and Air-Conditioning Engineers, Inc.

Qingyao Lu. 1987. HVAC DESIGN HANDBOOK. Beijing: China Architecture & Building Press.

816-852
Yuan Yuan, Xiaofeng Li and Yingxin Zhu. 2006. Experimental Study of Airflow in Naturally Ventilated Double Skin Facade, the Fourth International Symposium on Computational Wind Engineering, Japan
Yi Jiang, Yuanzhe Li and Hongfa Di. 1980. 关于透过体系透过率计算方法的探讨. Acta Energiae Slaris Sinica，Vol.1, No.2, pp166-175
DeST http://www.dest.com.cn